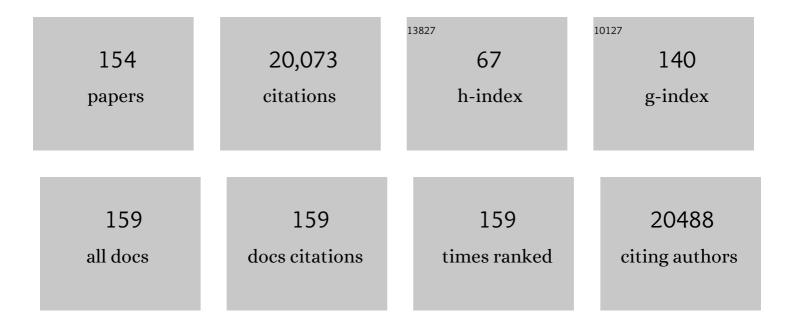
## Xudong Wang

List of Publications by Year in descending order

Source: https://exaly.com/author-pdf/7067211/publications.pdf Version: 2024-02-01



#	Article	IF	CITATIONS
1	Nucleation Kinetics and Structure Evolution of Quasi-Two-Dimensional ZnO at the Air–Water Interface: An <i>In Situ</i> Time-Resolved Grazing Incidence X-ray Scattering Study. Nano Letters, 2022, 22, 3040-3046.	4.5	7
2	Stretchable Encapsulation Materials with High Dynamic Water Resistivity and Tissue-Matching Elasticity. ACS Applied Materials & amp; Interfaces, 2022, 14, 18935-18943.	4.0	7
3	Highâ€Performance Poly(vinylidene difluoride)/Dopamine Core/Shell Piezoelectric Nanofiber and Its Application for Biomedical Sensors. Advanced Materials, 2021, 33, e2006093.	11.1	114
4	Wearable and Implantable Electroceuticals for Therapeutic Electrostimulations. Advanced Science, 2021, 8, 2004023.	5.6	73
5	Thickness-Dependent Piezoelectric Property from Quasi-Two-Dimensional Zinc Oxide Nanosheets with Unit Cell Resolution. Research, 2021, 2021, 1519340.	2.8	2
6	Bioresorbable Primary Battery Anodes Built on Core–Double-Shell Zinc Microparticle Networks. ACS Applied Materials & Interfaces, 2021, 13, 14275-14282.	4.0	10
7	Mechanisms of the Planar Growth of Lithium Metal Enabled by the 2D Lattice Confinement from a Ti <sub>3</sub> C <sub>2</sub> T <i><sub>x</sub></i> MXene Intermediate Layer. Advanced Functional Materials, 2021, 31, 2010987.	7.8	33
8	Wafer-scale heterostructured piezoelectric bio-organic thin films. Science, 2021, 373, 337-342.	6.0	129
9	A self-powered implantable and bioresorbable electrostimulation device for biofeedback bone fracture healing. Proceedings of the National Academy of Sciences of the United States of America, 2021, 118, .	3.3	71
10	Atomic layer deposition in the development of supercapacitor and lithium-ion battery devices. Carbon, 2021, 179, 299-326.	5.4	31
11	Materials Perspectives for Self-Powered Cardiac Implantable Electronic Devices toward Clinical Translation. Accounts of Materials Research, 2021, 2, 739-750.	5.9	16
12	Bulk Ferroelectric Metamaterial with Enhanced Piezoelectric and Biomimetic Mechanical Properties from Additive Manufacturing. ACS Nano, 2021, 15, 14903-14914.	7.3	21
13	A Rigid-Flexible Protecting Film with Surface Pits Structure for Dendrite-Free and High-Performance Lithium Metal Anode. Nano Letters, 2021, 21, 7063-7069.	4.5	24
14	Quasi-Two-Dimensional Earth-Abundant Bimetallic Electrocatalysts for Oxygen Evolution Reactions. ACS Energy Letters, 2021, 6, 3367-3375.	8.8	29
15	Accelerated complete human skin architecture restoration after wounding by nanogenerator-driven electrostimulation. Journal of Nanobiotechnology, 2021, 19, 280.	4.2	17
16	Nanogenerator for determination of acoustic power in ultrasonic reactors. Ultrasonics Sonochemistry, 2021, 78, 105718.	3.8	29
17	Long-term in vivo operation of implanted cardiac nanogenerators in swine. Nano Energy, 2021, 90, 106507.	8.2	19
18	Energy Harvesting Floor from Commercial Cellulosic Materials for a Self-Powered Wireless Transmission Sensor System. ACS Applied Materials & Interfaces, 2021, 13, 5133-5141.	4.0	37

#	Article	IF	CITATIONS
19	Self-powered liquid chemical sensors based on solid–liquid contact electrification. Analyst, The, 2021, 146, 1656-1662.	1.7	22
20	Confined Shear Alignment of Ultrathin Films of Cellulose Nanocrystals. ACS Applied Bio Materials, 2021, 4, 7961-7966.	2.3	5
21	Mesoporous Ultrathin In2O3 Nanosheet Cocatalysts on a Silicon Nanowire Photoanode for Efficient Photoelectrochemical Water Splitting. ACS Applied Materials & Interfaces, 2021, , .	4.0	10
22	Level-expansion: A statistical sequential design methodology with application to nanomaterial synthesis. Journal of Quality Technology, 2020, 52, 97-107.	1.8	0
23	Multifunctional Artificial Artery from Direct 3D Printing with Builtâ€In Ferroelectricity and Tissueâ€Matching Modulus for Realâ€Time Sensing and Occlusion Monitoring. Advanced Functional Materials, 2020, 30, 2002868.	7.8	46
24	<scp>Respirationâ€driven</scp> triboelectric nanogenerators for biomedical applications. EcoMat, 2020, 2, e12045.	6.8	58
25	Prevention of Hepatic Ischemia-Reperfusion Injury by Carbohydrate-Derived Nanoantioxidants. Nano Letters, 2020, 20, 6510-6519.	4.5	32
26	Two-dimensional nonlayered materials for electrocatalysis. Energy and Environmental Science, 2020, 13, 3993-4016.	15.6	76
27	In vitro study of enhanced photodynamic cancer cell killing effect by nanometer-thick gold nanosheets. Nano Research, 2020, 13, 3217-3223.	5.8	17
28	Phase transformation, charge transfer, and ionic diffusion of Na <sub>4</sub> MnV(PO <sub>4</sub> ) <sub>3</sub> in sodium-ion batteries: a combined first-principles and experimental study. Journal of Materials Chemistry A, 2020, 8, 17477-17486.	5.2	23
29	Piezoelectric Nanocellulose Thin Film with Large-Scale Vertical Crystal Alignment. ACS Applied Materials & Interfaces, 2020, 12, 26399-26404.	4.0	32
30	Implementation of ferroelectric materials in photocatalytic and photoelectrochemical water splitting. Nanoscale Horizons, 2020, 5, 1174-1187.	4.1	65
31	Non-contact cylindrical rotating triboelectric nanogenerator for harvesting kinetic energy from hydraulics. Nano Research, 2020, 13, 1903-1907.	5.8	97
32	Nanoparticle-Decorated Ultrathin La2O3 Nanosheets as an Efficient Electrocatalysis for Oxygen Evolution Reactions. Nano-Micro Letters, 2020, 12, 49.	14.4	51
33	Degradable piezoelectric biomaterials for wearable and implantable bioelectronics. Current Opinion in Solid State and Materials Science, 2020, 24, 100806.	5.6	87
34	Polymer-based Nanogenerator for Biomedical Applications. Chemical Research in Chinese Universities, 2020, 36, 41-54.	1.3	17
35	Tailored TiO <sub>2</sub> Protection Layer Enabled Efficient and Stable Microdome Structured pâ€GaAs Photoelectrochemical Cathodes. Advanced Energy Materials, 2020, 10, 1902985.	10.2	25
36	Memristive Behavior Enabled by Amorphous–Crystalline 2D Oxide Heterostructure. Advanced Materials, 2020, 32, e2000801.	11.1	26

#	Article	IF	CITATIONS
37	Bioinspired Synthesis of Quasi-Two-Dimensional Monocrystalline Oxides. Chemistry of Materials, 2019, 31, 9040-9048.	3.2	21
38	Enhanced Ferromagnetism from Organic–Cerium Oxide Hybrid Ultrathin Nanosheets. ACS Applied Materials & Interfaces, 2019, 11, 44601-44608.	4.0	8
39	Influences of screw dislocations on electroluminescence of AlGaN/AlN-based UVC LEDs. AIP Advances, 2019, 9, .	0.6	11
40	Self-Activated Electrical Stimulation for Effective Hair Regeneration <i>via</i> a Wearable Omnidirectional Pulse Generator. ACS Nano, 2019, 13, 12345-12356.	7.3	90
41	Massive Vacancy Concentration Yields Strong Room-Temperature Ferromagnetism in Two-Dimensional ZnO. Nano Letters, 2019, 19, 7085-7092.	4.5	31
42	Diethyl ether as self-healing electrolyte additive enabled long-life rechargeable aqueous zinc ion batteries. Nano Energy, 2019, 62, 275-281.	8.2	455
43	Effective anti-biofouling enabled by surface electric disturbance from water wave-driven nanogenerator. Nano Energy, 2019, 57, 558-565.	8.2	45
44	Germanium photodiodes on pyramidal textured surface by Metal-Assisted Chemical Etching. , 2019, , .		0
45	A wafer-scale 1 nm Ni(OH) <sub>2</sub> nanosheet with superior electrocatalytic activity for the oxygen evolution reaction. Nanoscale, 2018, 10, 5054-5059.	2.8	31
46	Computation of Electronic Energy Band Diagrams for Piezotronic Semiconductor and Electrochemical Systems. Advanced Electronic Materials, 2018, 4, 1700395.	2.6	15
47	AlGaAs/Si dualâ€junction tandem solar cells by epitaxial liftâ€off and printâ€transferâ€assisted direct bonding. Energy Science and Engineering, 2018, 6, 47-55.	1.9	12
48	Ionic Layer Epitaxy of Nanometer-Thick Palladium Nanosheets with Enhanced Electrocatalytic Properties. Chemistry of Materials, 2018, 30, 3308-3314.	3.2	29
49	Ultrathin Piezotronic Transistors with 2 nm Channel Lengths. ACS Nano, 2018, 12, 4903-4908.	7.3	63
50	Decoupling the charge collecting and screening effects in piezotronics-regulated photoelectrochemical systems by using graphene as the charge collector. Nano Energy, 2018, 48, 377-382.	8.2	14
51	H <sub>2</sub> V <sub>3</sub> O <sub>8</sub> Nanowire/Graphene Electrodes for Aqueous Rechargeable Zinc Ion Batteries with High Rate Capability and Large Capacity. Advanced Energy Materials, 2018, 8, 1800144.	10.2	427
52	VS <sub>4</sub> Nanoparticles Anchored on Graphene Sheets as a Highâ€Rate and Stable Electrode Material for Sodium Ion Batteries. ChemSusChem, 2018, 11, 735-742.	3.6	93
53	Implanted Battery-Free Direct-Current Micro-Power Supply from in Vivo Breath Energy Harvesting. ACS Applied Materials & Interfaces, 2018, 10, 42030-42038.	4.0	54
54	Effective weight control via an implanted self-powered vagus nerve stimulation device. Nature Communications, 2018, 9, 5349.	5.8	242

#	Article	IF	CITATIONS
55	Effective Wound Healing Enabled by Discrete Alternative Electric Fields from Wearable Nanogenerators. ACS Nano, 2018, 12, 12533-12540.	7.3	234
56	Surface Gradient Ti-Doped MnO <sub>2</sub> Nanowires for High-Rate and Long-Life Lithium Battery. ACS Applied Materials & Interfaces, 2018, 10, 44376-44384.	4.0	41
57	Piezotronic modulations in electro- and photochemical catalysis. MRS Bulletin, 2018, 43, 946-951.	1.7	52
58	Mesoporous carbon nanofiber network derived from agarose for supercapacitor electrode. Journal of Nanoparticle Research, 2018, 20, 1.	0.8	5
59	Enhanced Performance of Ge Photodiodes <i>via</i> Monolithic Antireflection Texturing and α-Ge Self-Passivation by Inverse Metal-Assisted Chemical Etching. ACS Nano, 2018, 12, 6748-6755.	7.3	50
60	Air-Flow-Driven Triboelectric Nanogenerators for Self-Powered Real-Time Respiratory Monitoring. ACS Nano, 2018, 12, 6156-6162.	7.3	229
61	Metastable Intermediates in Amorphous Titanium Oxide: A Hidden Role Leading to Ultra-Stable Photoanode Protection. Nano Letters, 2018, 18, 5335-5342.	4.5	36
62	Piezotronics in Photoâ€Electrochemistry. Advanced Materials, 2018, 30, e1800154.	11.1	44
63	Study of long-term biocompatibility and bio-safety of implantable nanogenerators. Nano Energy, 2018, 51, 728-735.	8.2	67
64	Ultrathin Surface Coating Enables Stabilized Zinc Metal Anode. Advanced Materials Interfaces, 2018, 5, 1800848.	1.9	476
65	Atomic Layer Deposition for Advanced Electrode Design in Photoelectrochemical and Triboelectric Systems. Advanced Materials Interfaces, 2017, 4, 1600835.	1.9	7
66	Hybrid graphene@MoS <sub>2</sub> @TiO <sub>2</sub> microspheres for use as a high performance negative electrode material for lithium ion batteries. Journal of Materials Chemistry A, 2017, 5, 3667-3674.	5.2	66
67	Wafer-scale synthesis of ultrathin CoO nanosheets with enhanced electrochemical catalytic properties. Journal of Materials Chemistry A, 2017, 5, 9060-9066.	5.2	31
68	Surface-Plasmon-Resonance-Enhanced Photoelectrochemical Water Splitting from Au-Nanoparticle-Decorated 3D TiO <sub>2</sub> Nanorod Architectures. Journal of Physical Chemistry C, 2017, 121, 12071-12079.	1.5	72
69	Chemically Functionalized Natural Cellulose Materials for Effective Triboelectric Nanogenerator Development. Advanced Functional Materials, 2017, 27, 1700794.	7.8	223
70	Simultaneous Enhancement of Charge Separation and Hole Transportation in a TiO <sub>2</sub> –SrTiO <sub>3</sub> Core–Shell Nanowire Photoelectrochemical System. Advanced Materials, 2017, 29, 1701432.	11.1	165
71	Research Update: Materials design of implantable nanogenerators for biomechanical energy harvesting. APL Materials, 2017, 5, .	2.2	68
72	Enhanced photoelectrochemical efficiency and stability using a conformal TiO2 film on a black silicon photoanode. Nature Energy, 2017, 2, .	19.8	217

#	Article	IF	CITATIONS
73	Single-crystalline germanium nanomembrane photodetectors on foreign nanocavities. Science Advances, 2017, 3, e1602783.	4.7	76
74	Celluloseâ€Based Nanomaterials for Energy Applications. Small, 2017, 13, 1702240.	5.2	189
75	Unit Cell Level Thickness Control of Single-Crystalline Zinc Oxide Nanosheets Enabled by Electrical Double-Layer Confinement. Langmuir, 2017, 33, 7708-7714.	1.6	24
76	Nature Degradable, Flexible, and Transparent Conductive Substrates from Green and Earth-Abundant Materials. Scientific Reports, 2017, 7, 4936.	1.6	34
77	Air-Stable Porous Fe <sub>2</sub> N Encapsulated in Carbon Microboxes with High Volumetric Lithium Storage Capacity and a Long Cycle Life. Nano Letters, 2017, 17, 5740-5746.	4.5	132
78	Hierarchical Branched Vanadium Oxide Nanorod@Si Nanowire Architecture for High Performance Supercapacitors. Small, 2017, 13, 1603076.	5.2	23
79	Inverted Wedding Cake Growth Operated by the Ehrlich–Schwoebel Barrier in Twoâ€Dimensional Nanocrystal Evolution. Angewandte Chemie - International Edition, 2016, 55, 2217-2221.	7.2	9
80	High-density platinum nanoparticle-decorated titanium dioxide nanofiber networks for efficient capillary photocatalytic hydrogen generation. Journal of Materials Chemistry A, 2016, 4, 11672-11679.	5.2	18
81	Piezoelectric and Triboelectric Dual Effects in Mechanical-Energy Harvesting Using BaTiO <sub>3</sub> /Polydimethylsiloxane Composite Film. ACS Applied Materials & Interfaces, 2016, 8, 34335-34341.	4.0	194
82	Calculation of the piezoelectric and flexoelectric effects in nanowires using a decoupled finite element analysis method. Journal of Applied Physics, 2016, 119, 154104.	1.1	8
83	Enhanced Photoelectrochemical Performance from Rationally Designed Anatase/Rutile TiO <sub>2</sub> Heterostructures. ACS Applied Materials & Interfaces, 2016, 8, 12239-12245.	4.0	147
84	Patterning at the 10 nanometer length scale using a strongly segregating block copolymer thin film and vapor phase infiltration of inorganic precursors. Nanoscale, 2016, 8, 11595-11601.	2.8	29
85	Triboelectric nanogenerators and power-boards from cellulose nanofibrils and recycled materials. Nano Energy, 2016, 30, 103-108.	8.2	185
86	Mesoporous Piezoelectric Polymer Composite Films with Tunable Mechanical Modulus for Harvesting Energy from Liquid Pressure Fluctuation. Advanced Functional Materials, 2016, 26, 6760-6765.	7.8	69
87	Biocompatibility and in vivo operation of implantable mesoporous PVDF-based nanogenerators. Nano Energy, 2016, 27, 275-281.	8.2	141
88	Semiconductor Nanowires for Energy Harvesting. Semiconductors and Semimetals, 2016, 94, 297-368.	0.4	9
89	Allâ€Textile Triboelectric Generator Compatible with Traditional Textile Process. Advanced Materials Technologies, 2016, 1, 1600147.	3.0	75
90	Directed self-assembly of block copolymer films on atomically-thin graphene chemical patterns. Scientific Reports, 2016, 6, 31407.	1.6	20

#	Article	IF	CITATIONS
91	Kinetics-Driven Crystal Facets Evolution at the Tip of Nanowires: A New Implementation of the Ostwald-Lussac Law. Nano Letters, 2016, 16, 7078-7084.	4.5	17
92	Inverted Wedding Cake Growth Operated by the Ehrlich–Schwoebel Barrier in Twoâ€Dimensional Nanocrystal Evolution. Angewandte Chemie, 2016, 128, 2257-2261.	1.6	3
93	Morphological control in the adaptive ionic layer epitaxy of ZnO nanosheets. Extreme Mechanics Letters, 2016, 7, 64-70.	2.0	14
94	Nanometre-thick single-crystalline nanosheets grown at the water–air interface. Nature Communications, 2016, 7, 10444.	5.8	133
95	Microwave TFTs Made of MOCVD ZnO With ALD Al2O3Gate Dielectric. IEEE Journal of the Electron Devices Society, 2016, 4, 55-59.	1.2	2
96	Chemical modification of polymer surfaces for advanced triboelectric nanogenerator development. Extreme Mechanics Letters, 2016, 9, 514-530.	2.0	160
97	Sequential Infiltration Synthesis of Doped Polymer Films with Tunable Electrical Properties for Efficient Triboelectric Nanogenerator Development. Advanced Materials, 2015, 27, 4938-4944.	11.1	159
98	Development of Lead Iodide Perovskite Solar Cells Using Three-Dimensional Titanium Dioxide Nanowire Architectures. ACS Nano, 2015, 9, 564-572.	7.3	125
99	Coupling of piezoelectric effect with electrochemical processes. Nano Energy, 2015, 14, 296-311.	8.2	153
100	Nitrogen Doped 3D Titanium Dioxide Nanorods Architecture with Significantly Enhanced Visible Light Photoactivity. Journal of Physical Chemistry C, 2015, 119, 4397-4405.	1.5	37
101	Single-electrode triboelectric nanogenerator for scavenging friction energy from rolling tires. Nano Energy, 2015, 15, 227-234.	8.2	151
102	Wedding Cake Growth Mechanism in One-Dimensional and Two-Dimensional Nanostructure Evolution. Nano Letters, 2015, 15, 7766-7772.	4.5	43
103	Ferroelectric Polarization-Enhanced Photoelectrochemical Water Splitting in TiO <sub>2</sub> –BaTiO <sub>3</sub> Core–Shell Nanowire Photoanodes. Nano Letters, 2015, 15, 7574-7580.	4.5	280
104	Piezotronic-Enhanced Photoelectrochemical Reactions in Ni(OH) <sub>2</sub> -Decorated ZnO Photoanodes. Journal of Physical Chemistry Letters, 2015, 6, 3410-3416.	2.1	67
105	Cellulose nanofiber-templated three-dimension TiO <sub>2</sub> hierarchical nanowire network for photoelectrochemical photoanode. Nanotechnology, 2014, 25, 504005.	1.3	34
106	Photoelectrodes: Highly Efficient Capillary Photoelectrochemical Water Splitting Using Cellulose Nanofiberâ€Templated TiO <sub>2</sub> Photoanodes (Adv. Mater. 14/2014). Advanced Materials, 2014, 26, 2110-2110.	11.1	4
107	Spongeâ€Like Piezoelectric Polymer Films for Scalable and Integratable Nanogenerators and Selfâ€Powered Electronic Systems. Advanced Energy Materials, 2014, 4, 1301624.	10.2	326
108	Significant performance enhancement of ZnO photoanodes from Ni(OH)2 electrocatalyst nanosheets overcoating. Nano Energy, 2014, 6, 10-18.	8.2	76

#	Article	IF	CITATIONS
109	Evolution of Hollow TiO <sub>2</sub> Nanostructures via the Kirkendall Effect Driven by Cation Exchange with Enhanced Photoelectrochemical Performance. Nano Letters, 2014, 14, 2528-2535.	4.5	113
110	Enhanced photoresponse of ZnO nanorods-based self-powered photodetector by piezotronic interface engineering. Nano Energy, 2014, 9, 237-244.	8.2	193
111	One-Dimensional Titanium Dioxide Nanomaterials: Nanowires, Nanorods, and Nanobelts. Chemical Reviews, 2014, 114, 9346-9384.	23.0	601
112	Mechanisms in the solution growth of free-standing two-dimensional inorganic nanomaterials. Nanoscale, 2014, 6, 6398.	2.8	57
113	Cl-Doped ZnO Nanowires with Metallic Conductivity and Their Application for High-Performance Photoelectrochemical Electrodes. ACS Applied Materials & Interfaces, 2014, 6, 1288-1293.	4.0	80
114	Highly Efficient Capillary Photoelectrochemical Water Splitting Using Cellulose Nanofiberâ€Templated TiO <sub>2</sub> Photoanodes. Advanced Materials, 2014, 26, 2262-2267.	11.1	104
115	Electron Microscopy Observation of TiO <sub>2</sub> Nanocrystal Evolution in High-Temperature Atomic Layer Deposition. Nano Letters, 2013, 13, 5727-5734.	4.5	49
116	Spatial modeling for refining and predicting surface potential mapping with enhanced resolution. Nanoscale, 2013, 5, 921.	2.8	8
117	Mapping of strain–piezopotential relationship along bent zinc oxide microwires. Nano Energy, 2013, 2, 1225-1231.	8.2	10
118	Spontaneous Phase Transformation and Exfoliation of Rectangular Single-Crystal Zinc Hydroxy Dodecylsulfate Nanomembranes. ACS Nano, 2013, 7, 6007-6016.	7.3	17
119	Evolution of titanium dioxide one-dimensional nanostructures from surface-reaction-limited pulsed chemical vapor deposition. Journal of Materials Research, 2013, 28, 270-279.	1.2	17
120	Piezoelectricâ€Polarizationâ€Enhanced Photovoltaic Performance in Depletedâ€Heterojunction Quantumâ€Dot Solar Cells. Advanced Materials, 2013, 25, 916-921.	11.1	96
121	Fundamental Analysis of Piezocatalysis Process on the Surfaces of Strained Piezoelectric Materials. Scientific Reports, 2013, 3, 2160.	1.6	169
122	Fabrication and Characterization of Si/GaInP Heterojunction Photodetectors. , 2012, , .		0
123	Substrate-Free Self-Assembly Approach toward Large-Area Nanomembranes. ACS Nano, 2012, 6, 2602-2609.	7.3	38
124	Piezoelectric nanogenerators—Harvesting ambient mechanical energy at the nanometer scale. Nano Energy, 2012, 1, 13-24.	8.2	410
125	Hierarchical TiO2–Si nanowire architecture with photoelectrochemical activity under visible light illumination. Energy and Environmental Science, 2012, 5, 7918.	15.6	57
126	Band Structure Engineering at Heterojunction Interfaces via the Piezotronic Effect. Advanced Materials, 2012, 24, 4683-4691.	11.1	111

#	Article	IF	CITATIONS
127	Piezopotentialâ€Driven Redox Reactions at the Surface of Piezoelectric Materials. Angewandte Chemie - International Edition, 2012, 51, 5962-5966.	7.2	251
128	Threeâ€Dimensional Kelvin Probe Microscopy for Characterizing Inâ€Plane Piezoelectric Potential of Laterally Deflected ZnO Microâ€∕Nanowires. Advanced Functional Materials, 2012, 22, 652-660.	7.8	24
129	Three-Dimensional High-Density Hierarchical Nanowire Architecture for High-Performance Photoelectrochemical Electrodes. Nano Letters, 2011, 11, 3413-3419.	4.5	223
130	Growth of Rutile Titanium Dioxide Nanowires by Pulsed Chemical Vapor Deposition. Crystal Growth and Design, 2011, 11, 949-954.	1.4	98
131	PVDF microbelts for harvesting energy from respiration. Energy and Environmental Science, 2011, 4, 4508.	15.6	287
132	Growth of Titanium Dioxide Nanorods in 3D-Confined Spaces. Nano Letters, 2011, 11, 624-631.	4.5	79
133	Interface Engineering by Piezoelectric Potential in ZnO-Based Photoelectrochemical Anode. Nano Letters, 2011, 11, 5587-5593.	4.5	131
134	Highâ€Performance Integrated ZnO Nanowire UV Sensors on Rigid and Flexible Substrates. Advanced Functional Materials, 2011, 21, 4464-4469.	7.8	293
135	Piezoelectric Nanogenerators for Mechanical Energy Harvesting. International Symposium on Microelectronics, 2011, 2011, 000367-000375.	0.3	0
136	Fundamental study of mechanical energy harvesting using piezoelectric nanostructures. Journal of Applied Physics, 2010, 108, .	1.1	124
137	Waferâ€Level Patterned and Aligned Polymer Nanowire/Micro―and Nanotube Arrays on any Substrate. Advanced Materials, 2009, 21, 2072-2076.	11.1	52
138	Output of an ultrasonic wave-driven nanogenerator in a confined tube. Nano Research, 2009, 2, 177-182.	5.8	25
139	Nanowire Structured Hybrid Cell for Concurrently Scavenging Solar and Mechanical Energies. Journal of the American Chemical Society, 2009, 131, 5866-5872.	6.6	182
140	Microfibre–nanowire hybrid structure for energy scavenging. Nature, 2008, 451, 809-813.	13.7	1,480
141	Piezoelectric Nanogenerators for Self-Powered Nanodevices. IEEE Pervasive Computing, 2008, 7, 49-55.	1.1	72
142	Integrated Nanogenerators in Biofluid. Nano Letters, 2007, 7, 2475-2479.	4.5	155
143	Direct-Current Nanogenerator Driven by Ultrasonic Waves. Science, 2007, 316, 102-105.	6.0	2,065
144	Nanowire and nanobelt arrays of zinc oxide from synthesis to properties and to novel devices. Journal of Materials Chemistry, 2007, 17, 711.	6.7	261

#	Article	IF	CITATIONS
145	High-performance pentacene field-effect transistors using Al2O3 gate dielectrics prepared by atomic layer deposition (ALD). Organic Electronics, 2007, 8, 718-726.	1.4	133
146	Piezoelectric Field Effect Transistor and Nanoforce Sensor Based on a Single ZnO Nanowire. Nano Letters, 2006, 6, 2768-2772.	4.5	983
147	Density-Controlled Growth of Aligned ZnO Nanowires Sharing a Common Contact:  A Simple, Low-Cost, and Mask-Free Technique for Large-Scale Applications. Journal of Physical Chemistry B, 2006, 110, 7720-7724.	1.2	120
148	Controlled Replication of Butterfly Wings for Achieving Tunable Photonic Properties. Nano Letters, 2006, 6, 2325-2331.	4.5	475
149	Self-attraction among aligned Au/ZnO nanorods under electron beam. Applied Physics Letters, 2005, 86, 013111.	1.5	69
150	Growth of Uniformly Aligned ZnO Nanowire Heterojunction Arrays on GaN, AlN, and Al0.5Ga0.5N Substrates. Journal of the American Chemical Society, 2005, 127, 7920-7923.	6.6	244
151	Large-Size Liftable Inverted-Nanobowl Sheets as Reusable Masks for Nanolithiography. Nano Letters, 2005, 5, 1784-1788.	4.5	61
152	Large-Scale Synthesis of Six-Nanometer-Wide ZnO Nanobelts. Journal of Physical Chemistry B, 2004, 108, 8773-8777.	1.2	295
153	Large-Scale Hexagonal-Patterned Growth of Aligned ZnO Nanorods for Nano-optoelectronics and Nanosensor Arrays. Nano Letters, 2004, 4, 423-426.	4.5	1,477
154	The morphology of cast zinc-based alloy reinforced by spheroidal silicon phase and its wear resistance. International Journal of Cast Metals Research, 1998, 11, 39-42.	0.5	1